SMC-TR-93-15

AEROSPACE REPORT NO.
TR-0091(6945-03)-1

Photoelectron Spectroscopy of MoS_2 at the Sulfur 2p Absorption Edge

Prepared by

S. V. DIDZIULIS and J. R. LINCE
Mechanics and Materials Technology Center
Technology Operations

D. K. SHUH, T. D. DURBIN, and J. A. YARMOFF
Department of Physics
University of California, Riverside

15 October 1992

Prepared for

SPACE AND MISSILE SYSTEMS CENTER
AIR FORCE MATERIEL COMMAND
Los Angeles Air Force Base
P. O. Box 92960
Los Angeles, CA 90009-2960

Engineering and Technology Group

THE AEROSPACE CORPORATION
El Segundo, California

This report was submitted by The Aerospace Corporation, El Segundo, CA 90245-4691, under Contract No. F04701-88-C-0089 with the Space and Missile Systems Center, P. O. Box 92960, Los Angeles, CA 90009-2960. It was reviewed and approved for The Aerospace Corporation by R. W. Fillers, Principal Director, Mechanics and Materials Technology Center. Capt. Mark Borden was the project officer for the Mission-Oriented Investigation and Experimentation (MOIE) program.

This report has been reviewed by the Public Affairs Office (PAS) and is releasable to the National Technical Information Service (NTIS). At NTIS, it will be available to the general public, including foreign nationals.

This technical report has been reviewed and is approved for publication. Publication of this report does not constitute Air Force approval of the report's findings or conclusions. It is published only for the exchange and stimulation of ideas.

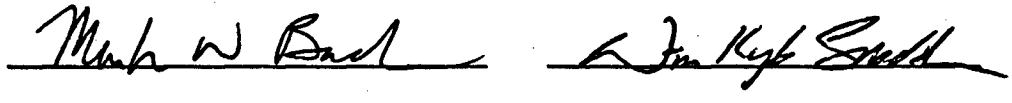

UNCLASSIFIED

SECURITY CLASSIFICATION OF THIS PAGE

REPORT DOCUMENTATION PAGE

1a. REPORT SECURITY CLASSIFICATION Unclassified	1b. RESTRICTIVE MARKINGS
2a. SECURITY CLASSIFICATION AUTHORITY	3. DISTRIBUTION/AVAILABILITY OF REPORT Approved for public release; distribution unlimited
2b. DECLASSIFICATION/DOWNGRADING SCHEDULE	
4. PERFORMING ORGANIZATION REPORT NUMBER(S) TR-0091(6945-03)-1	5. MONITORING ORGANIZATION REPORT NUMBER(S) SMC-TR-93-15
6a. NAME OF PERFORMING ORGANIZATION The Aerospace Corporation Technology Operations 6b. OFFICE SYMBOL (If applicable)	7a. NAME OF MONITORING ORGANIZATION Space and Missile Systems Center
6c. ADDRESS (City, State, and ZIP Code) El Segundo, CA 90245-4691	7b. ADDRESS (City, State, and ZIP Code) Los Angeles Air Force Base Los Angeles, CA 90009-2960
8a. NAME OF FUNDING/SPONSORING ORGANIZATION 8b. OFFICE SYMBOL (If applicable)	9. PROCUREMENT INSTRUMENT IDENTIFICATION NUMBER F04701-88-C-0089
8c. ADDRESS (City, State, and ZIP Code)	10. SOURCE OF FUNDING NUMBERS PROGRAM ELEMENT NO. / PROJECT NO. / TASK NO. / WORK UNIT ACCESSION NO.

11. TITLE (Include Security Classification)

Photoelectron Spectroscopy of MoS_2 at the Sulfur 2p Absorption Edge

12. PERSONAL AUTHOR(S)

Didziulis, Stephen V.; and Lince, Jeffrey R.

13a. TYPE OF REPORT	13b. TIME COVERED FROM ____ TO ____	14. DATE OF REPORT (Year, Month, Day)	15. PAGE COUNT
		1992 October 15	28

16. SUPPLEMENTARY NOTATION

17. COSATI CODES			18. SUBJECT TERMS (Continue on reverse if necessary and identify by block number)
FIELD	GROUP	SUB-GROUP	Photoelectron spectroscopy, Molybdenum disulfide, Solid lubricant, Resonant photoelectron spectroscopy

19. ABSTRACT (Continue on reverse if necessary and identify by block number)

The sulfur 2p absorption edge and valence band resonant photoelectron spectra of molybdenum disulfide (MoS_2), obtained using synchrotron radiation, are compared to the Mo 4p edge results from previous work. A pre-edge feature in the S 2p data shows transitions to unoccupied, dominantly Mo 4d antibonding levels, indicating that significant covalent interactions exist between Mo and S valence orbitals. Resonant enhancement of valence band photoelectron shake-up peaks is observed at the S 2p → Mo 4d excitation energies, while the sulfur $L_{2,3}VV$ Auger peak dominates the spectrum when the S 2p ionization threshold is reached. Antiresonant intensity modulation of main valence band peaks is observed at photon energies corresponding to the S 2p → Mo 4d pre-edge feature. The results show that the principal decay channel after the S 2p→ Mo 4d excitation leads to the enhancement of final states having S $3p^4$ Mo $4d^3$ electron configurations.

20. DISTRIBUTION/AVAILABILITY OF ABSTRACT	21. ABSTRACT SECURITY CLASSIFICATION
[X] UNCLASSIFIED/UNLIMITED [ ] SAME AS RPT. [ ] DTIC USERS	Unclassified

22a. NAME OF RESPONSIBLE INDIVIDUAL	22b. TELEPHONE (Include Area Code)	22c. OFFICE SYMBOL

DD FORM 1473, 84 MAR

83 APR edition may be used until exhausted.
All other editions are obsolete.

SECURITY CLASSIFICATION OF THIS PAGE

UNCLASSIFIED

PREFACE

This work was supported by Air Force Systems Command, Space Systems Division Contract No. F04701-88-C-0089. Data were obtained at the National Synchrotron Light Source, Brookhaven National Laboratory, Upton, New York, which is supported by the U. S. Department of Energy, Division of Materials Sciences and Division of Chemical Sciences (DOE Contract No. DE-AC02-76CH00016). We thank Dr. F. R. McFeely and Dr. L. J. Terminello of IBM Thomas J. Watson Research Center and the staff at NSLS for their assistance. One of us (SVD) thanks Dr. P. D. Fleischauer of The Aerospace Corporation and Prof. K. D. Butcher of California Lutheran University for helpful discussions.

CONTENTS

FIGURES

I. INTRODUCTION

Molybdenum disulfide (MoS_2) is the most widely used solid lubricant for space applications. The unique geometric and electronic structure of MoS_2 provide its unique lubricating properties. This report details part of an ongoing program aimed at understanding the fundamental electronic structure and bonding of MoS_2 and relating these properties to the layered compound's friction, wear, and adhesion characteristics. These results will provide insight for further experimental study of film chemistry and guide theoretical work on the bonding and lubrication properties of MoS_2. The work described herein details a new technique for examining valence orbital bonding interactions that could easily be extended to other inorganic compounds.

X-ray absorption edge and valence band resonant photoelectron spectroscopic (PES) studies on transition metal compounds are usually conducted at a metal-core-level excitation.[1-6] The soft X-ray absorption near edge structure of such compounds normally shows transitions from the metal-core-level (often np) to unoccupied, predominantly metal-based valence levels [nd and (n+1)s], revealing, to some degree, the nature and splitting of these levels. Resonant photoemission at metal edges allows the assignment of the final state electronic configuration of valence band photoelectron peaks through the intensity enhancement of final states containing metal orbital character. Little work has been performed on ligand-core-level excitations of transition metal compounds and resulting resonance effects. This report explores this area by comparing the S 2p absorption edge of molybdenum disulfide (MoS_2) to the Mo 4p edge and examines valence band resonance effects near the S 2p edge.

The valence band electronic structure of MoS_2 has been studied in detail with PES[7-11] and resonant PES at the Mo 4p absorption edge.[12] The rich, highly resolved structure of the valence band has generated fairly well-documented peak assignments, which will be discussed in the Results section.[7-12] The high resolution of MoS_2 valence band spectra should allow the effects of the S 2p edge resonance processes on particular final states to be determined, a rare opportunity in the PES of solids.

The studies near the S 2p edge were pursued to further explore the electronic structure of MoS_2 and to complement our previous work, particularly that done at the Mo 4p edge. Previous work on transition metal compounds has shown that ligand core level → unoccupied metal valence level transitions can occur when significant covalent mixing of ligand and metal valence states exists.[13, 14] Some work has been performed on nonmetal 2p soft X-ray absorption edges, including two reports of the S $L_{2,3}$ edge in MoS_2.[15,16] A limited number of resonant PES studies have been reported at nonmetal edges,[17-21] but no reports of nonmetal edge resonances in transition metal compounds have been made. PES studies performed on gas-phase compounds such as SiF_4[18,19] and SF_6[20] have shown enhancement of shake-up satellites rather than main-band features at the Si and S 2p edges, respectively. Alternatively, resonant PES of BF_3 showed enhancement of main-band features as well as shake-ups at the B 1s edge.[21] If resonant enhancement of ligand-based valence band features commonly occurs at nonmetal edges in transition metal compounds, then new avenues of investigation could be opened for determining electronic structures of these materials. Differences in bonding interactions in metal compounds, such as the admixture of metal character into the ligand valence levels, could change valence

electron repulsion phenomena and alter relaxation pathways observed for similar edges in gas-phase compounds. MoS_2 is an ideal compound for such a study because the valence band features are well resolved, allowing the detection of small intensity changes of peaks representing well-defined final states.

The present work has three goals, all involving the use of synchrotron radiation to examine effects at the S 2p absorption edge. The first goal is to use the S 2p edge to explore the unoccupied conduction band states of MoS_2 to provide a more complete picture of the electronic structure of this material. The second goal is to examine resonant effects on the valence band PES features at photon energies near the S 2p edge. The final goal is to compare the results obtained at the S 2p edge to those obtained at the Mo 4p edge in MoS_2 and to other non-metal absorption edge studies to evaluate the utility of ligand edge techniques in the study of the electronic structure of transition metal compounds.

II. EXPERIMENTAL

Photoelectron spectra were obtained at beam line UV-8b at the National Synchrotron Light Source at Brookhaven National Laboratory, Upton, New York. The toroidal grating beam line monochromator[22] and high-resolution electron spectrometer[23] have been described in detail elsewhere. Briefly, the spectrometer collects angle-integrated data with a sample collection solid angle of ~ $\pi/2$ sr, centered approximately about the surface normal. Valence band spectra, therefore, are measured as an average over the MoS_2 Brillouin zone. To normalize spectra to the incident photon flux, the sample signal was divided by the total current resulting from electron emission from the gold-coated beam line final refocusing mirror. The mirror current was detected with an electrometer. All binding energies are reported relative to the spectrometer Fermi level.

Photoelectron spectra were obtained at photon energies of 150 to 250 eV, and data were collected by signal averaging with a spectrometer pass energy of 30 eV. Constant final state (CFS) data were obtained with partial electron yield by monitoring the intensity of electrons in the secondary electron tail in a 0.5 eV wide window centered at 20 eV kinetic energy. For CFS spectra, the pass energy was increased to 50 eV to increase signal intensity.

Clean (0001) MoS_2 surfaces were produced by cleavage in air of natural crystals (Wards Natural Science Establishment, Rochester, New York), followed by annealing at approximately 1125 K for 20 min in a sample preparation chamber with a base pressure of 1×10^{-10} torr. This annealing procedure has been shown to produce clean, defect-free (0001) surfaces.[24, 25] Following the anneal, the sample was transferred to the spectrometer chamber (base pressure $<1 \times 10^{-10}$ torr) under ultrahigh vacuum, and data were taken immediately. The sample was judged fit for use if sharp Mo 3d, S 2p core-level and valence-band spectra were obtained. There was no evidence of any oxygen, carbon, or other contaminants on the sample surface.

III. RESULTS

A. MoS_2 VALENCE ELECTRONIC STRUCTURE

Figure 1 shows the MoS_2 valence-band spectrum obtained with a photon energy of 250 eV. The peak at lowest binding energy results from photoemission of Mo 4d electrons. This assignment is based on a comparison of the photon energy-dependent peak intensity changes to theoretical photoionization cross sections and the strong resonant enhancement of this peak at the Mo 4p → 4d edge.[7-12] The remaining valence band features result from photoemission from S-based valence levels. The highest binding energy valence feature near 15 eV is the S 3s PES peak, while the peaks ranging from 7 to 3 eV are dominantly S 3p emissions that are split by bonding interactions with unoccupied Mo 4d, 5s, and 5p orbitals. The two lower binding energy S 3p peaks near 4 and 5 eV are resonantly enhanced at the Mo 4p edge, indicating that these final states have significant Mo 4d character mixed into them.

The PES valence-band assignments are generally in agreement with other experimental[26-29] and theoretical[8, 9, 26, 27, 30] electronic structure studies of MoS_2. In addition, the distinct peak splittings have shown good agreement with a molecular orbital (MO) energy level description.[30] A qualitative MO energy-level diagram for an MoS_2 cluster having D_{3h} symmetry (the site symmetry for Mo in MoS_2) and the resulting PES peak assignments are also shown in Fig. 1. The $2a_1'$ (Mo $4d_{z^2}$) level is the highest occupied MO, consistent with the assignment of the lowest binding energy peak. The S 3p-based 1e' and 1e" orbitals are shown as the next highest occupied levels, based on the resonant enhancement of the low binding energy S 3p peaks previously discussed. The 1e' and 1e" orbitals are formed through mixing with Mo 4d orbitals and, hence, have antibonding, dominantly metal counterparts that are the lowest unoccupied MOs (2e' and 2e").[31] The diagram shows the S 3p-based $1a_1'$ and $1a_2''$ levels (with arbitrary relative ordering), assigned as the two highest binding energy S 3p peaks. The higher binding energy core levels (S 3s, Mo 4p, and S 2p) and the unoccupied Mo 4d, 5s, and 5p levels are also included.

B. THE S 2p EDGE

Figure 2 compares the S 2p CFS spectrum to the Mo 4p CFS spectrum from our earlier work.[12] In agreement with previous work,[15] the S 2p edge (Fig. 2b) shows two distinct regions, a small pre-edge feature at photon energies of 162.5 to 166.5 eV and an intense feature starting at 167.5 eV and continuing past 175 eV. The measured binding energy for the S 2p levels in MoS_2 (162.3 eV) places the final states achieved in the pre-edge feature (shown in detail in Fig. 2c) just above the Fermi level for the n-type semiconductor, ignoring final-state relaxation changes. These transition energies lead to the assignment of the pre-edge feature as transitions from the S 2p level to bound, antibonding levels having dominantly Mo 4d character in the MO picture. The S 2p edge data is more highly resolved than the same region of the Mo 4p edge (Fig. 2a), indicating that the S 2p feature is better suited for determining the density of unoccupied conduction-band states in MoS_2.

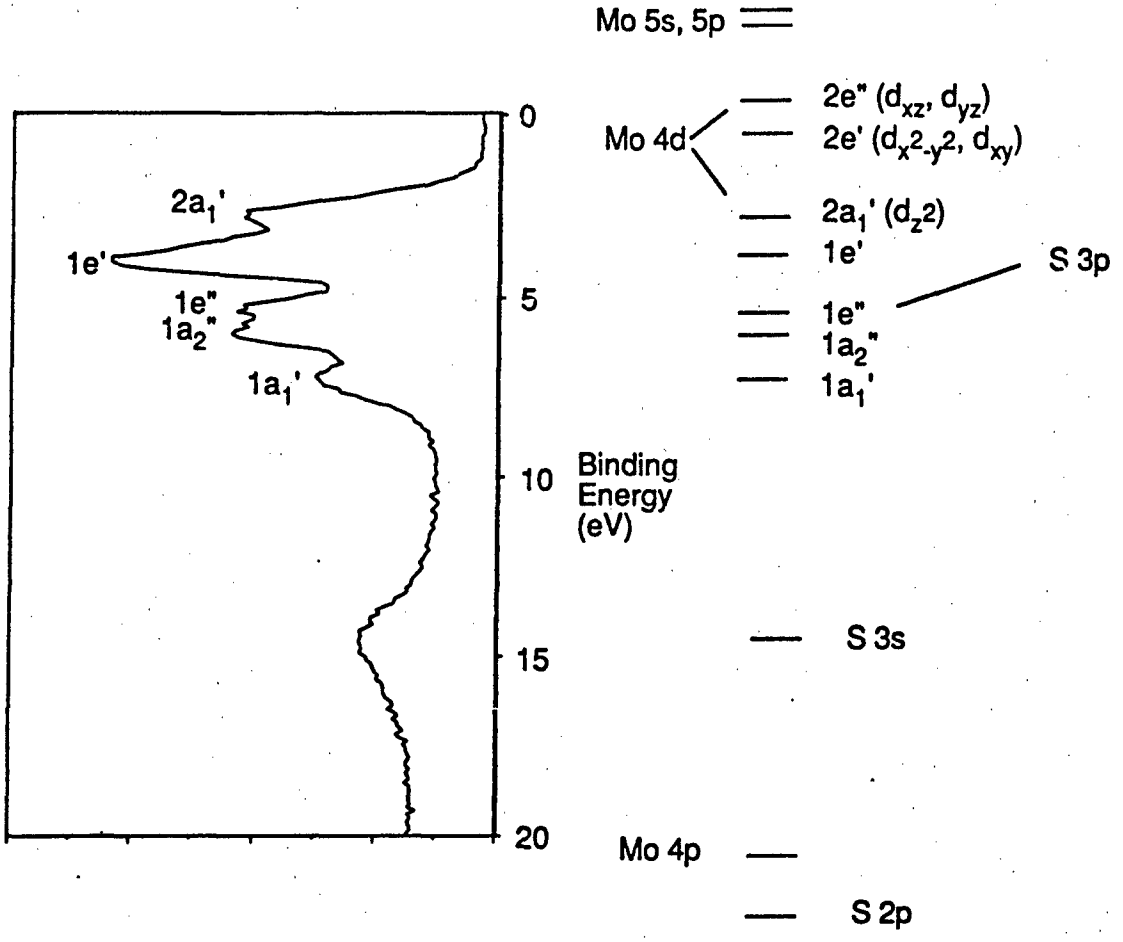

Figure 1. Valence band PES spectrum of MoS_2 obtained at 250 eV photon energy with peaks labeled as assigned using a molecular orbital model. A qualitative molecular orbital energy-level diagram for MoS_2 in a cluster having D_{3h} symmetry is shown at the right.

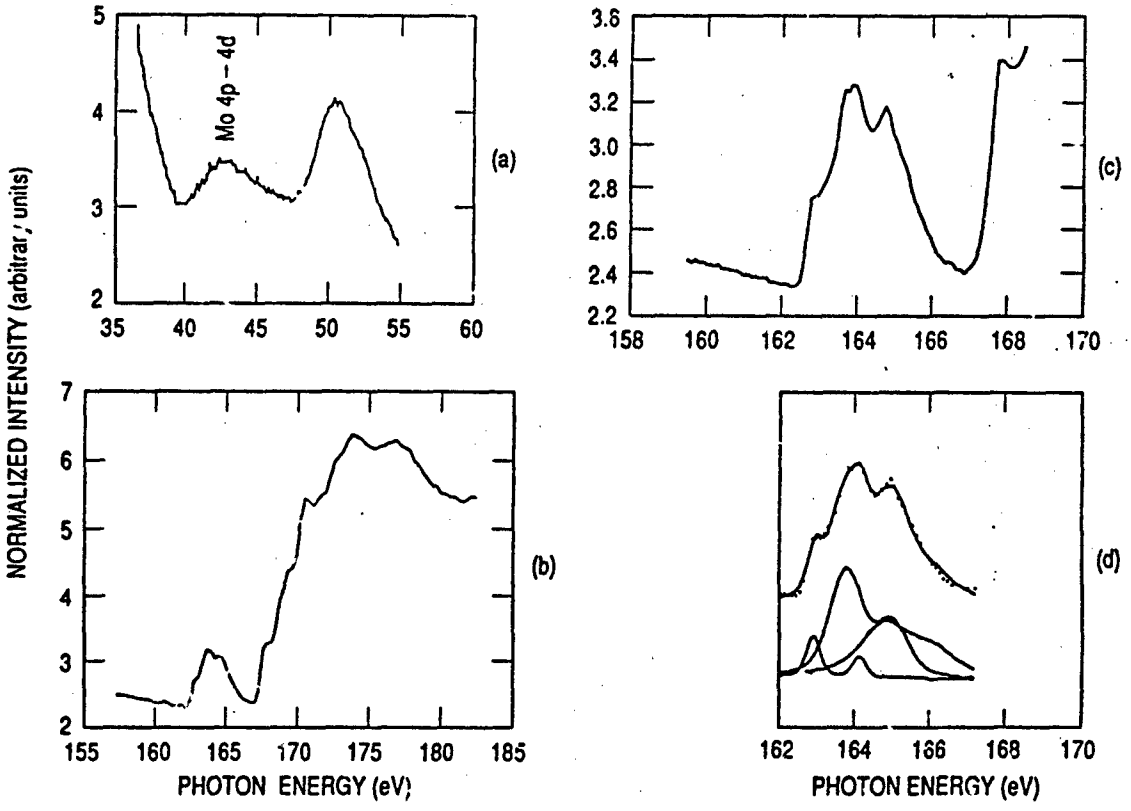

Figure 2. Constant Final State spectra of MoS_2 obtained at (a) the Mo 4p absorption edge and (b) the S 2p absorption edge. (c) The pre-edge feature at the S 2p edge is shown in more detail along with (d) the best fit to this region using three spin-orbit split Gaussian pairs.

The threshold energy of the remaining large edge feature (167.5 eV) corresponds closely to the ionization threshold for S 2p electrons (S 2p binding energy + work function). Hence, this feature must be dominated by transitions to states above the ionization threshold energy. Sharp peaks are observed on the broad band that have been attributed to transitions to higher energy bound states,[16] or more recently to photoelectron scattering processes.[15] The energy separation of this broad feature relative to the S 2p → Mo 4d transitions corresponds roughly to the higher energy peak seen in the Mo 4p edge. The Mo 4p edge feature was assigned as having contributions from transitions to higher, unoccupied Mo orbitals (5s and 5p), based on the resonant enhancement of Mo 4d-containing valence band features observed at these photon energies.[12]

Our interest in this work lies primarily in the pre-edge feature shown in detail in Fig. 2c, which contains transitions to the Mo 4d-based antibonding (conduction band) states. Sonntag and Brown observed a similar feature using X-ray absorption techniques. They fit the pre-edge region with a pair of spin-orbit split ($E_{s.o.}$ = 1.15 eV) Gaussians, indicating two transitions to the conduction band (to the 2e' and 2e" levels in Fig. 1) with S $2p_{3/2}$ maxima at 162.8 eV and 164 4 eV.[16]

$$S(2p)^6\cdots(2a_1')^2(d_{z^2}) \rightarrow S(2p)^5\cdots(2a_1')^2(2e')^1[d_{x^2-y^2}, d_{xy}] \quad (1a)$$

$$\rightarrow S(2p)^5\cdots(2a_1')^2(2e')^1[d_{xz}, d_{yz}] \quad (1b)$$

Each transition having a final state with a hole in the S 2p level is spin-orbit split into the $2p_{3/2}$ and $2p_{1/2}$ states.

Our CFS peak shape is slightly different from the absorption spectrum of Sonntag and Brown and needed three spin-orbit split ($E_{s.o.}$ = 1.19 eV)[24] Gaussian pairs for a reasonable fit, indicating the presence of three dominant transitions with S $2p_{3/2}$ component transition energies of 162.9, 163.7, and 164.7 eV. The fit is shown in Fig. 2d, where the two higher energy transitions have approximately equal integrated intensities: the 163.7 eV doublet is about 1.3 times more intense than the 164.7 eV doublet, and both transitions are much more intense (by a factor of 5) than the 162.9 eV transition.

C. RESONANT PHOTOEMISSION

The MoS_2 valence-band PES data obtained at photon energies near the S 2p edge are given in Figs. 3 and 4. In Fig. 3, the valence band spectra have the normal shape expected for MoS_2 at photon energies below the edge (152.5 and 160.5 eV), with the exception of the two sharp peaks moving to lower binding energy as the photon energy is increased. These moving peaks are the S $2p_{3/2,1/2}$ ionizations excited by second-order radiation from the monochromator. The second-order peaks make it difficult to detect any subtle intensity changes in the valence band region (i.e., by comparing the 160.5 eV spectrum to spectra obtained with higher photon energies). However, these peaks provide a convenient method of determining the final-state energy position achieved by the excitation of S 2p electrons by first-order radiation. In Fig. 3, the location of the Fermi level is indicated by the dashed line to show when the S 2p electrons have sufficient energy to reach conduction-band states.

In the S 2p CFS spectrum of Fig. 2b, the threshold of the pre-edge excitation feature is at approximately 162.5 eV. The valence-band spectrum at this photon energy is shown in Fig. 3. In this spectrum, the second-order S $2p_{3/2}$ peak is about 1 eV above the valence-band maximum, nearly overlapping the Fermi level. Subtle variations exist in the 162.5 eV spectrum compared to the 160.5 eV spectrum (aside from the movement of the second-order peaks). These variations can be observed in difference spectra that will be discussed subsequently and in a direct data comparison. In the direct comparison, a small intensity increase on the low binding energy side of the S 3s peak is observed.

As shown in Fig. 3, when the photon energy is further increased, significant changes are observed in the vicinity of the S 3s peak. At 163.0 eV, a large intensity increase is observed in a broad binding energy region from ~ 9 to 15 eV, with the maximum on the low binding energy side of the S 3s peak. The 163.0 eV photon energy corresponds to the first shoulder in the CFS spectrum in Fig. 3b. When the photon energy is increased to 163.5 eV, the enhancement in the S 3s region increases further, with the broad intensity maximum still under the S 3s. In the 164.0 eV valence-band spectrum (near the second peak in the CFS spectrum), the nature of the resonant

effect changes slightly as the enhanced peak is broadened to higher binding energy. Similar enhancement in the 9 to 15 eV region is observed at 164.5 eV. However, the intensity is lower at 164.5 eV than at 164.0 eV, corresponding to a dip in the CFS intensity at this photon energy. The final peak in the CFS pre-edge feature is observed at 164.8 eV, and the spectrum taken at 164.8 eV is given in Fig. 3. The intensity of the enhanced region has increased over that obtained at 164.5 eV, showing that the resonant enhancement follows the CFS profile. When the photon energy is further increased to 165.5 and 166.0 eV, moving off the S 2p → Mo 4d CFS feature, the enhancement again wanes and shifts to higher binding energy.

In spectra taken in the valley between the main CFS features, at photon energies of 166.5 and 167 eV, a small shoulder is observed on the high binding energy side of the S 3s in Fig. 4. This shoulder grows dramatically and shifts to a higher binding energy (staying at a constant kinetic energy of 145 eV) as the photon energy is increased into the second, larger CFS feature. The intense, constant kinetic energy peak arising in the valence-band data results from the S $L_{2,3}VV$ Auger decay, which is allowed above the S 2p ionization threshold.

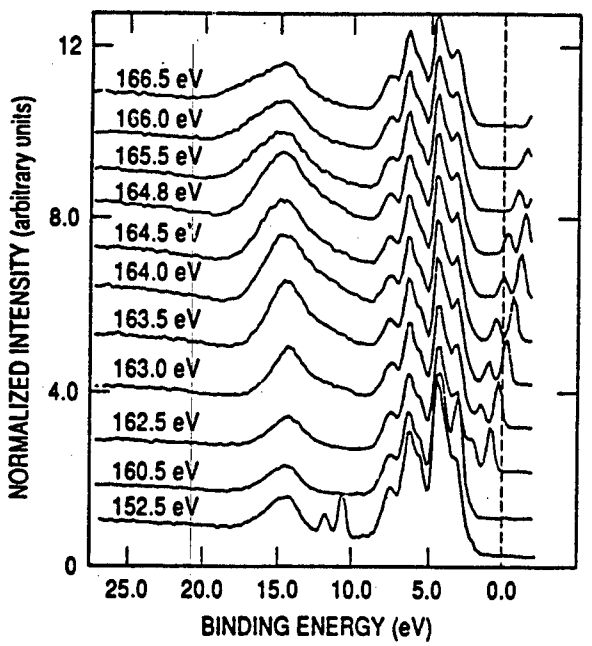

Figure 3. Normalized valence band PES data for MoS_2 obtained near the S 2p absorption edge. The photon energies at which spectra were obtained are listed on the figure. S $2p_{3/2,1/2}$ ionizations excited by second-order light are evident near 11 and 12 eV in the 152.5-eV data. The Fermi level is indicated by the broken line at 0.0 eV binding energy on the right of the figure. Spectra were normalized by dividing by the photoelectron current detected on the beamline refocusing mirror.

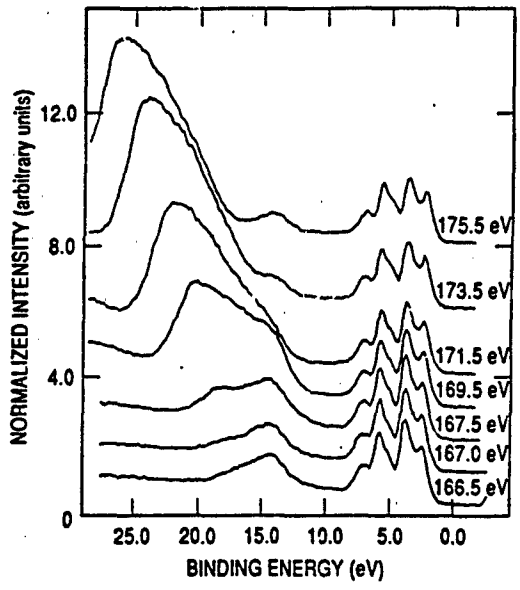

Figure 4. Normalized valence band PES for MoS_2 obtained at the photon energies listed on the figure. The photon energies correspond to the large CFS feature indicative of transitions to continuum states.

The changes observed in the valence-band features were further investigated through difference spectra obtained by subtracting the 160.5 eV data from the spectra obtained at higher energies. These difference spectra are presented in Fig. 5, with the photon energy of the higher energy spectrum listed on the figure. Concentrating on the 9 to 15 eV binding energy region, we observe an intensity increase at 13 eV binding energy in the 162.5-eV threshold data. In the 163.0-eV spectrum, a broad region of enhancement is evident, extending from approximately 8 to 15 eV binding energy. The maximum is again located in the region of the S 3s peak but has shifted to higher binding energy compared to the 162.5-eV data. As the excitation energy is increased to 163.5 eV, the enhancement maximum shifts to slightly higher binding energy and remains broad and asymmetric. The enhancement maximum remains fixed at a binding energy of −14.5 eV for the 164.0-eV data, but the peak broadens toward higher binding energy. At 164.5 and 164.8 eV, the intensity maximum is again shifted to slightly higher binding energy, and in the 164.8-eV data, enhancement is observed over a 10-eV energy range. In the photon energy range of 163.0 to 164.8 eV, the intensity maximum in the resonant enhancement shifts to higher binding energy by only 0.5 eV. Therefore, the resonantly enhanced feature is not simply an Auger peak remaining at constant kinetic energy. As the photon energy is increased to 165.5, 166.0, and 166.5 eV, the resonant enhancement shifts to higher binding energy, decreases in intensity, and occurs over a narrower binding energy region.

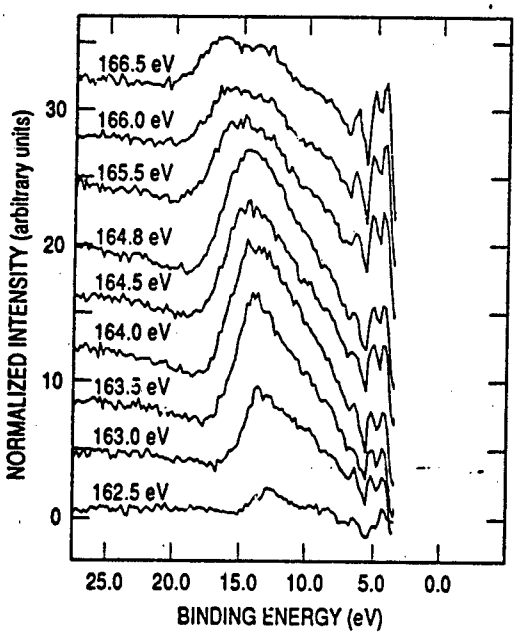

Figure 5. Valence band difference spectra for MoS_2 as a function of photon energy. Spectra were generated by subtracting the 160.5-eV data from the data obtained at the photon energies listed on the spectra. The low binding energy portions of the spectra have been removed to eliminate areas influenced by the S 2p second-order peaks.

Intensity changes in the main-band PES peaks through the S 2p edge region were quite difficult to follow due to the presence of the second-order S 2p peaks in the 160.5 eV data and the significant intensity increases between the S 3s and main valence region at resonance. These problems confounded attempts to fit the valence data with Gaussian peaks to follow any subtle intensity changes. It can be safely stated that no dramatic intensity enhancements occur in the main band. There are, however, important changes that can be documented by careful comparison of spectra.

Overall, there is a significant decrease in the absolute normalized intensity of all main valence-band features at the edge. The normalized, total integrated intensity of the 164.0-eV spectrum main-band features is only ~60% of that at 152.5 eV. This decrease is much greater than that expected from simple cross-section changes in this photon energy region.[32]

On closer examination of the spectra at resonance, intensity changes differ for particular valence-band peaks. A small dip in intensity of the two highest binding energy, S 3p-based, main-band features (assigned as $1a_1'$ and $1a_2''$) occurs at 162.5 eV relative to 160.5 eV. This dip is followed by a slight intensity increase at the S 2p → Mo 4d transition energies of 163 to 165 eV, but this finding is highly tentative due to apparent background changes. At the higher photon energies in the S 2p → Mo 4d region, there is a definite intensity decrease in valence-band peaks having dominantly S 3p character. The difference spectra in Fig. 5 show larger dips in the 4- to 7-eV binding energy region with increasing photon energy.

Finally, Fig. 6 compares the main valence-band regions obtained at 152.5, 164.0, and 250 eV normalized to the intensity of the Mo 4d feature at lowest binding energy. At the height of the

resonance in Fig. 6b (164.0 eV), the two lowest binding energy S 3p peaks, indicated on the figure, show significant intensity decreases relative to the remainder of the valence band when compared to data obtained well below the edge (152.5 eV) in Fig. 6a. These peaks have been assigned as ionization of the 1e' and 1e" levels, the bonding counterparts to the 2e' and 2e" Mo 4d-based levels to which the S 2p electrons are being excited. In the 250 eV data shown in Fig. 6c, well past the effects of the S 2p edge, the valence-band spectrum more closely resembles the 152.5-eV data than the 164-eV data. The absolute valence-band intensity decrease indicates that the entire valence band is displaying an anti-resonance at the S 2p edge, but the effects are greatest in bonding counterparts to the shake-up final state 2e' and 2e" levels.

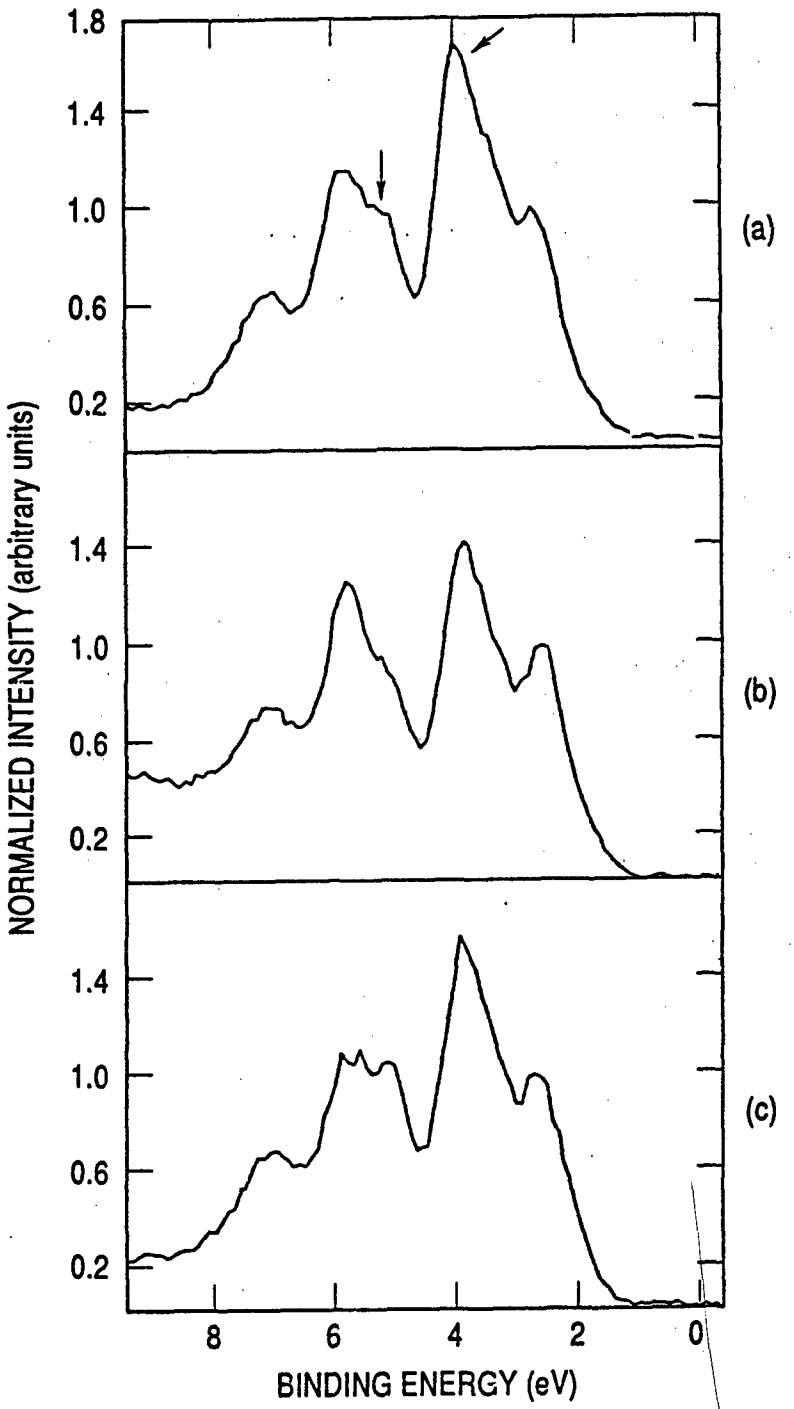

Figure 6. Valence band spectra for MoS_2 taken at photon energies of (a) 152 eV, (b) 164 eV, and (c) 250 eV, showing only the main band features. The spectra have been normalized to the intensity of the lowest binding energy feature (Mo $4d_{z}2$). Note the intensity decrease of the two lowest binding energy S 3p features [indicated by arrows in part (a)] relative to the other valence band peaks at resonance in the 164 eV data.

IV. DISCUSSION

A. THE S 2p EDGE

The CFS spectrum obtained at the S 2p edge gives a higher-resolution picture of the conduction-band density of states than does the Mo 4p edge. The very sharp, well-defined S 2p core-level energy in MoS_2 contributes to the high-resolution S 2p edge. In addition, differences in final-state relaxation phenomena related to the location of the final-state core hole on the S atom might contribute to the increased spectral resolution.

Absorption edge phenomena of transition metal compounds are often described in atomic pictures, particularly at metal edges involving final states with large exchange interactions.[6] Such a picture is difficult to describe for the S 2p edge of MoS_2, where the atomic transitions must be viewed as occurring from the S 2p core level to the S 3p valence levels. However, atomic selection rules and the formally filled $3p^6$ subshell of the sulfide ion preclude these transitions. These transitions should be discussed using the MO electronic configurations as written in Eqs. 1(a) and (b), where the pre-edge feature represents transitions from the S 2p core level to Mo 4d-based molecular orbitals having S 3p admixture.

The observation of the S 2p → Mo 4d transition indicates that significant covalent mixing between the Mo 4d and S 3p valence levels exists in MoS_2, a finding that confirms the observed resonance effects in S-based features in previous work.[12] In the MO picture of Fig. 1, two unoccupied Mo 4d-based (conduction band) energy levels exist, the 2e' and 2e". The nearly equal integrated intensities of the 163.7- and 164.7-eV CFS peaks lead to their tentative assignment as transitions to the 2e' and 2e" states. The 2e'-2e" splitting should be similar to that observed in the occupied 1e'-1e" valence band PES peaks (0.8 eV)[12] if only S 3p-Mo 4d bonding interactions are considered.[4] Our CFS fit gives a 1.0 eV splitting, which is closer to the 1e'-1e" splitting than the fit of Sonntag and Brown (1.6 eV).[16] Configuration interactions with the Mo 5p-based 3e' level would tend to shift the 2e' and 1e' levels downward in Fig. 1, resulting in relatively smaller 1e'-1e" and larger 2e'-2e" splittings.

If the two intense CFS transitions are viewed as the S 2p → 2e' and 2e", then the higher energy transition must be considered as the 2e". The theoretically higher covalency in the 2e" state predicts the higher energy transition to have greater intensity,[14] which is clearly in disagreement with our results (and also with the fit of Sonntag and Brown). An alternative explanation for our CFS fit that would be consistent with covalency arguments is the assignment of the 162.9-eV peak as the e' transition and the 163.7-eV peak as the e" transition. This assignment, however, fails to explain the significant intensity of the 164.7-eV feature.

The CFS peak intensities and the presence of a third transition probably represent a limitation of a one-electron, MO picture in the description of the electronic structure of extended lattice systems. In a band structure calculation for MoS_2, two regions with high densities of states corresponding to the 2e' and 2e" MO levels are predicted with an additional feature at lower energies resulting from K_5 band states.[33] Transitions to this K_5 state could produce the sharp 162.9-eV component in our CFS fit. The broad peaks needed to fit the remainder of the CFS spectrum

could be the result of dispersion of the conduction-band states. The predicted higher covalency of the 2e" should lead to a greater energy dispersion of the band resulting from these states, leading to the observed broad absorption feature.

B. RESONANT PHOTOEMISSION

The two regions observed in the S 2p CFS data of Fig. 2b produce two distinctly different effects in the valence-band PES of MoS_2. At photon energies above the 167.0-eV threshold of the larger edge feature, the intense, constant kinetic energy S $L_{2,3}VV$ Auger peak is observed. This is consistent with these photons having sufficient energy to ionize the S 2p electrons, with the core hole relaxing through the production of an Auger electron.

The resonant intensity changes occurring at photon energies corresponding to the pre-edge feature are more subtle. The most likely cause of the intensity increase in the S 3s region from 9 to 15 eV is the enhancement of shake-up final states. These final states would be achieved through a similar auto-ionization pathway as the Auger peak just discussed; however, the electron excited at the edge remains in an excited state, acting as a spectator in the decay. For example, excitation to the 2e' antibonding level

$$S(2p)^6\cdots(1a_1')^2(1a_2'')^2(1e')^4(1e'')^4(2a_1')^2 \rightarrow S(2p)^5\cdots(1a_1')^2(1a_2'')^2(1e')^4(1e'')^4(2a_1')^2(2e')^1 \quad (2)$$

allows for several possible decay modes involving the electrons in the S 3p-based MOs, leading to shake-up final states. This process can be demonstrated more simply in an atomic picture:

excitation $\quad S\ (2p)^6\ldots\ S\ (3p)^6\ Mo\ (4d)^2 \rightarrow S\ (2p)^5\ldots\ S\ (3p)^6\ Mo\ (4d)^3 \quad (3a)$

auto-ionization $\quad S\ (2p)^5\ldots\ S\ (3p)^6\ Mo\ (4d)^3 \rightarrow S\ (2p)^6\ldots\ S\ (3p)^4\ Mo\ (4d)^3 + e^-_{vac} \quad (3b)$

This decay path enhances photoemission features with final-state energies that correspond to the ionization of a S 3p electron plus the excitation of a S 3p electron to a conduction-band state. In general, these excited final states should be located at binding energies higher than the valence-band S 3p-based molecular orbital ($1a_1', 1a_2'', 1e', 1e''$) ionization final states, which is the region in which we observe enhancement. The enhanced region is broad due to the wide variety of possible final states involving all of the occupied S 3p molecular orbitals.

The lack of large enhancements of any main valence-band features indicates that several other possible decay modes are minor or nonexistent. For example, at the Mo 4p edge, the decay of the $4d^3$ excited state was achieved by the following process:

$$Mo\ (4p)^6\ldots\ Mo\ (4d)^2 \rightarrow\ Mo\ (4p)^5\ldots\ Mo\ (4d)^3 \rightarrow\ Mo\ (4p)^6\ldots\ Mo\ (4d)^1 + e^-_{vac} \quad (4)$$

This mechanism led to the enhancement of main-band features having d^1 final-state character.[12] Clearly, there is no significant enhancement of d^1 final state character at the S 2p edge, which would affect the lowest binding energy ($2a_1'$) peak. This lack of enhancement eliminates an interatomic Auger decay mechanism (5) as a possible channel.

$$S\ (2p)^6 \ldots\ Mo\ (4d)^2 \rightarrow S\ (2p)^5 \ldots\ Mo\ (4d)^3 \xrightarrow{-X} S\ (2p)^6 \ldots\ Mo\ (4d)^1 + e^-_{vac} \qquad (5)$$

A decay mechanism that would enhance S 3p-based valence-band peaks would require a S $3p^5$ final state:

$$S\ (2p)^6 \ldots\ S\ (3p)^6\ Mo\ (4d)^2 \rightarrow S\ (2p)^5 \ldots\ S\ (3p)^6\ Mo\ (4d)^3 \rightarrow \qquad (6)$$

$$S\ (2p)^6 \ldots\ S\ (3p)^5\ Mo\ (4d)^2 + e^-_{vac}$$

This could be a minor pathway in our study, as some modulation of the S 3p-based valence-band features was observed. However, as discussed previously, these intensity changes were complicated by changes in background and may be artifacts. In fact, the overall intensity decrease of all main valence-band features indicates that they are experiencing an antiresonance at the S 2p → Mo 4d edge, which is expected when shake-up peaks are excited.[3] The most interesting aspect of the antiresonance is the greater intensity decrease seen in the 1e' and 1e" peaks, as shown in Fig. 6. These same peaks showed significant enhancement at the Mo 4p edge.[12] The greater antiresonance in these peaks appears to result because the S 2p electrons are being excited to the antibonding counterparts (2e' and 2e") of these levels in the conduction band.

The enhancement of shake-up states in the region of the S 3s peak make the possible enhancement of $3s^1$ final states difficult to address. However, this decay channel is not observed in similar experiments on Ar,[34] which has a filled 3p shell (analogous to a sulfide ion). The difference spectra in Fig. 5 show an initial enhancement at lower binding energy than the S 3s peak and a broad region of enhanced final states at higher photon energies, proving that final states other than the S $3s^1$ are being enhanced.

In Fig. 5, the maximum in resonant intensity enhancement in each difference spectrum moves to higher binding energy, and the enhancement changes shape with increasing photon energy. This phenomenon occurs because higher energy shake-up final states can be reached as the photon energy is increased through the edge. The shake-up intensity maximum shifts in a step-like fashion, remaining at an essentially constant binding energy from 163.0 to 164.0 eV, before shifting in the 164.5 and 164.8 eV data, consistent with the transitions to the different final states observed in the CFS. The entire range of the shake-up states covers a region approximately 10 eV wide, which should be compared to the LVV Auger peak in the 173.5 eV spectrum of Fig. 4, which is quite broad and covers approximately 10 eV at its base. The shake-up peak shape at its

resonance maximum closely resembles that of the Auger peak because the decay mechanisms are closely related.

Resonant enhancement of shake-up final states in MoS_2 indicates that the decay mechanism of the excited sulfide species is dominated by Coulomb repulsion in the full S 3p-based valence orbitals. The electron excited to the Mo-based antibonding level acts as a spectator in the decay process. Shake-up enhancement is also observed at the S and Si 2p edges in SF_6 and SiF_4, compounds[17-20] in which the excited central atom should be electron deficient relative to S in MoS_2, decreasing the effective Coulomb repulsion. Alternatively, enhancement of both F-based σ-bonding main-band features and shake-up satellites occurs after excitation of a B 1s electron in BF_3.[21] Coulomb repulsions of B 2p electrons should be greater than for third-row species,[35] perhaps causing the excited electron to participate in the decay. Non-metal resonance decay processes, therefore, can proceed by a variety of pathways.

The resonance process in MoS_2 is fundamentally different from the gas-phase fluorides just described. In the fluorides, the excitation is occurring on the central non-metal atom, which is less electronegative than its fluoride ligands, a fact that results in the presence of unoccupied valence orbitals on the excited atom. Therefore, all edge transitions are occurring to antibonding orbitals centered on the excited atom, and the decay pathways to produce shake-up enhancement must proceed via an inter-atomic Auger mechanism. Coulomb repulsion is quite high for valence electrons on F atoms (formally F^-),[35] perhaps facilitating the observed decay processes. In MoS_2, the edge excitations occur from the S 2p core level to Mo-based molecular orbitals, and the decay occurs solely on the S atom. The effects of covalent bonding and Coulomb repulsion in the Mo 4d-based orbitals appear less significant than the Coulomb repulsion in the sulfur 3p-based MOs but are still influential in the antiresonance of the e' and e" main-band features. There is, however, need for theoretical treatments of the excitation and decay processes related to charge transfer and inter-atomic Auger decay mechanisms.

V. SUMMARY

The S 2p absorption edge and valence band resonant PES at the S 2p edge have been used to further understand the electronic structure of MoS_2. The S 2p edge revealed transitions to bound states best described as molecular orbitals having predominantly Mo 4d character but mixed with S 3p character, providing a charge transfer pathway. In addition, a larger feature dominated by transitions to states above the vacuum level was also observed. The S 2p edge was much better resolved than similar features obtained previously at the Mo 4p edge, allowing a clearer picture of the splitting of antibonding levels (conduction band density of states) to develop.

Valence band resonant PES obtained at the S 2p $\rightarrow$ Mo 4d excitation energy showed enhancement of shake-up satellite peaks located between 8 and 15 eV binding energy. These peaks likely represent final states equivalent to the ionization of electrons from the S 3p-based molecular orbitals plus the charge transfer of an electron from a S 3p level to a Mo 4d level. The lack of significant resonant enhancement of main valence peaks indicates that the decay channels that would produce these final states are minor compared to the shake-up decay pathway. In fact, antiresonant behavior is indicated by intensity decreases of all main-band features, with the predominantly S 3p 1e' and 1e" MOs, which have significant Mo 4d final-state character, showing the greatest effect. At photon energies above the S 2p ionization threshold, the S $L_{2,3}VV$ Auger peak grows to dominate the spectrum.

The antiresonant behavior of particular main valence band features related to the shake-up final states indicates that this technique has some utility in the assignment of main valence band PES features, particularly if pertinent metal edges are unavailable for study. The technique is also useful in probing excited PES final states that are not usually observed in normal PES experiments. Different results might be obtained for transition metal compounds having greater d electron-electron repulsion, which could enhance decay pathways involving the metal d-electrons instead of just those centered on the ligand atom.

REFERENCES

1. I. Fujimori and F. Minami, ***Phys. Rev. B,*** **30** (1984) 957.
2. M. R. Thuler, R. L. Benbow, and Z. Hurych, ***Phys. Rev.*** **B, 27** (1983) 2082.
3. L. C. Davis, ***J. Appl. Phys.,*** **59** (1986) R25 and references therein.
4. S. V. Didziulis, S. L. Cohen, K. D. Butcher, and E. I. Solomon, ***Inorg. Chem.,*** **27** (1988) 2238.
5. S. V. Didziulis, S. L. Cohen, A. A. Gewirth, and E. I. Solomon, ***J. Am. Chem. Soc.,*** **110** (1988) 250.
6. K. D. Butcher, S. V. Didziulis, B. Briat, and E. I. Solomon, ***J. Am. Chem. Soc.,*** **112** (1990) 2231.
7. J. C. McMenamin and W. E. Spicer, ***Phys. Rev. Lett.,*** **29** (1972) 1501.
8. R. Coehoorn, C. Haas, J. Dijkstra, C. J. Flipse, R. A. De Groot, and A. Wold, ***Phys. Rev. B,*** **35** (1987) 6195.
9. R. Mamy, A. Boufelja, and B. Carricaburu, ***Phys. Status Solidi B,*** **141** (1987) 467.
10. I. Abbati, L. Braicovich, C. Carbone, J. Nogami, I. Lindau, and U. del Pennino, ***J. Elect. Spectrosc. Relat. Phenom.,*** **40** (1986) 353.
11. I. T. McGovern, K. D. Childs, H. M. Clearfield, and R. H. Williams, ***J. Phys. C,*** **14** (1981) L243.
12. J. R. Lince, S. V. Didziulis, and J. A. Yarmoff, ***Phys. Rev. B.,*** **43** (1991) 4641.
13. B. Hedman, P. Frank, S. F. Gheller, W. E. Newton, E. I. Solomon, and K. O. Hodgson, ***Physica B,*** **158** (1989) 71.
14. B. Hedman, K. O. Hodgson, and E. I. Solomon, ***J. Am. Chem. Soc.,*** **112** (1990) 1643.
15. M. Kasraj, M. E. Fleet, T. K. Sham, G. M. Bancroft, K. H. Tan, and J. R. Brown, ***Solid State Commun.,*** **68** (1988) 507.
16. B. Sonntag and F. C. Brown, ***Phys. Rev. B,*** **10** (1974) 2300.
17. K. L. I. Kobayashi, H. Daimon, and Y. Murata, ***Phys. Rev. Lett.,*** **50** (1983) 1701.
18. S. Aksela, K. H. Tan, H. Aksela, and G. M. Bancroft, ***Phys. Rev. A,*** **33** (1986) 258.
19. T. A. Ferrett, M. N. Piancastelli, D. W. Lindle, P. A. Heimann, and D. A. Shirley, ***Phys. Rev. A,*** **38** (1988) 701.

20. T. A. Ferrett, D. W. Lindle, P. A. Heimann, M. N. Piancastelli, P. H. Kobrin, H. G. Kerkhoff, U. Becker, W. D. Brewer, and D. A. Shirley, ***J. Chem. Phys.,*** **89** (1988) 4726.

21. H. Kanamori, S. Iwata, A Mikuni, and T Sasaki, ***J. Phys. B: At. Mol. Phys.,*** **17** (1984) 3887.

22. D. E. Eastman, J. J. Donelon, N. C. Hien, and F. J. Himpsel, ***Nucl. Instrum. Methods,*** **172** (1980) 327.

23. F. J. Himpsel, Y. Jugnet, D. E. Eastman, J. J. Donelon, D. Grimm, G. Landgren, A. Marx, J. F. Morar, C. Oden, and R. A. Pollak, ***Nucl. Instrum. Methods,*** **222** (1984) 107.

24. J. R. Lince, T. B. Stewart, M. M. Hills, P. D. Fleischauer, J. A. Yarmoff, and A. Taleb-Ibrahimi, ***Surf. Sci.,*** **210** (1989) 387.

25. J. R. Lince, T. B. Stewart, M. M. Hills, P. D. Fleischauer, J. A. Yarmoff, and A. Taleb-Ibrahimi, ***Surf. Sci.,*** **223** (1989) 65.

26. A. Simunek and G. Wiech, ***Phys. Rev. D,*** **30** (1984) 923.

27. D. E. Haycock, D. S. Urch, and G. Wiech, ***Faraday Trans. II,*** **75** (1979) 1692.

28. Y. Ohno, K. Hirama, S. Nakai, C. Suguira, and S. Okada, ***Phys. Rev. B,*** **27** (1983) 3811.

29. Y. Ohno, K. Hirama, S. Nakai, C. Suguira, and S. Okada, ***J. Phys C,*** **16** (1983) 6695.

30. P. D. Fleischauer, J. R. Lince, P. A Bertrand, and R. Bauer, ***Langmuir,*** **5** (1989) 1009.

31. The relative ordering of 1e' and 1e" levels has not been determined experimentally, although the e" MOs (mixed with d_{xz} and d_{yz}) should have greater overlap of ligand and metal atomic orbitals than the e' (mixed with $d_{x^2-y^2}$ and d_{xy}) because the S ligands are out of the xy plane. Greater overlap should lead to a larger bonding interaction, stabilizing the 1e" to higher binding energy.

32. J. J. Yeh and I. Lindau, ***At. Data Nucl. Data Tables,*** **32** (1985) 1.

33. L. F. Mattheiss, ***Phys. Rev. B,*** **8** (1973) 3719.

34. H. Aksela, S. Aksela, H. Pulkkinen, G. M. Bancroft, and K. H. Tan, ***Phys. Rev.*** **A, 37** (1988) 1798.

35. W. A. Harrison, ***Phys. Rev. B,*** **31** (1985) 2121.

TECHNOLOGY OPERATIONS

The Aerospace Corporation functions as an "architect-engineer" for national security programs, specializing in advanced military space systems. The Corporation's Technology Operations supports the effective and timely development and operation of national security systems through scientific research and the application of advanced technology. Vital to the success of the Corporation is the technical staff's wide-ranging expertise and its ability to stay abreast of new technological developments and program support issues associated with rapidly evolving space systems. Contributing capabilities are provided by these individual Technology Centers:

Electronics Technology Center: Microelectronics, solid-state device physics, VLSI reliability, compound semiconductors, radiation hardening, data storage technologies, infrared detector devices and testing; electro-optics, quantum electronics, solid-state lasers, optical propagation and communications; cw and pulsed chemical laser development, optical resonators, beam control, atmospheric propagation, and laser effects and countermeasures; atomic frequency standards, applied laser spectroscopy, laser chemistry, laser optoelectronics, phase conjugation and coherent imaging, solar cell physics, battery electrochemistry, battery testing and evaluation.

Mechanics and Materials Technology Center: Evaluation and characterization of new materials: metals, alloys, ceramics, polymers and their composites, and new forms of carbon; development and analysis of thin films and deposition techniques; nondestructive evaluation, component failure analysis and reliability; fracture mechanics and stress corrosion; development and evaluation of hardened components; analysis and evaluation of materials at cryogenic and elevated temperatures; launch vehicle and reentry fluid mechanics, heat transfer and flight dynamics; chemical and electric propulsion; spacecraft structural mechanics, spacecraft survivability and vulnerability assessment; contamination, thermal and structural control; high temperature thermomechanics, gas kinetics and radiation; lubrication and surface phenomena.

Space and Environment Technology Center: Magnetospheric, auroral and cosmic ray physics, wave-particle interactions, magnetospheric plasma waves; atmospheric and ionospheric physics, density and composition of the upper atmosphere, remote sensing using atmospheric radiation; solar physics, infrared astronomy, infrared signature analysis; effects of solar activity, magnetic storms and nuclear explosions on the earth's atmosphere, ionosphere and magnetosphere; effects of electromagnetic and particulate radiations on space systems; space instrumentation; propellant chemistry, chemical dynamics, environmental chemistry, trace detection; atmospheric chemical reactions, atmospheric optics, light scattering, state-specific chemical reactions and radiative signatures of missile plumes, and sensor out-of-field-of-view rejection.